JKAU: Earth Sci., **Vol. 20**, No. 2, pp: 45-69 (2009 A.D. / 1430 A.H.)

Role of Argillic Alteration in Uranophane Precipitation along Shear Zones of the Gattar Granites, Eastern Desert, Egypt

Hamdy Hamed Abd El-Naby*

Nuclear Materials Authority, P.O. 530 El-Maadi, Cairo, Egypt
E-mail: hhabdel@yahoo.com

Received: 20/8 /2008 Accepted: 25/2/2009

Abstract. To study uranophane precipitation in the shear zones of the Gattar granites, X-ray diffraction (XRD), Back Scattered Electron imaging (BSE), Wavelength-Dispersion Spectral scan (WDS), X-ray compositional mapping and quantitative Electron Probe Micro Analyses (EPMA) were performed on uranophane, kaolinite and illite separated from these zones. Secondary uranium mineralization is controlled by shear zones in which the degree of fluid-rock interaction was very high and argillic alteration is abundant. The argillic alteration, represented mainly by kaolinite and illite, played an important role in uranophane precipitation within the altered parts of the Gattar granites. Presence of calcite as void-filling in association with uranophane within the shear zones of Gattar granites may indicate that uranium was probably transported as uranyl-carbonate complexes. The sorption of U(VI) in the Gattar clay minerals should be low due to the presence of dissolved carbonate ions and to the slightly alkaline conditions under which U(VI) occurs as the weakly sorbed $UO_2(CO_3)_3^{4-}$. U could be removed from solution through dissolution of feldspar, formation of clay minerals and subsequent precipitation of uranophane. Dissolution of the feldspars resulted in a diffusional gradient of Ca and SiO_4 ions away from its surface. Formation of uranophane would likely form near the clay minerals surface, where there was increased probability of successful interaction between U and both Ca and SiO_4. As the uranium loading increases, surface-precipitation of uranophane on clay mineral surfaces can occur.

Keywords: Gattar, granite, uranophane, alteration, kaolinite, illite.

*Present address: King Abdulaziz University, Faculty of Earth Sciences, P.O. Box 80206 Jeddah 21589, Saudi Arabia.

Introduction

The high specific surface area, low permeability, high sorption capacity, abundance in natural superficial environments and the ability to adsorb cations of clay minerals make them of crucial importance for radionuclide retention in natural systems (Meunier and Velde, 1998; Akçay, 1998; and Gaskova and Bukaty, 2008). Therefore, these clay minerals influence remarkably the physico-chemical properties of geological formations where they are present. Moreover, they could be used for a large variety of environmental applications such as water purification, highly radioactive waste treatment, mineral barriers for waste landfill, and slurry walls for the encapsulation of contaminated areas. Uranium in natural waters is predominantly found as U(VI) in the stable uranyl form $(UO_2)^{2+}$, which starts hydrolyzing above pH 4 and is the predominant species in solution up to pH 5. Under atmospheric conditions and above pH 7, U(VI) carbonate complexes become predominant in aqueous solution (Wazne *et al.*, 2004).

Uranium mineralization in Gattar granites is structurally controlled and associated with quartz veinlets. These granites exhibit extensive alteration, including Na- and K-metasomatism, silicification, argillization, chloritization, and pyritization (Salman *et al.*, 1986; Helmy, 1999; and El-Kammar *et al.*, 2001). Mass balance calculations by El-Kammar *et al.* (2001) indicate loss of Si, Be, Rb, REE and remarkable gain of U, Y and transition elements, due to both Na- and K-metasomatism.

Over the last 20 years, particular attention has been paid by many researchers to get information on the conditions of mobilization and retention of radionuclides in geological formations, especially igneous and clayey formations (Chapman, 1994; Hidaka and Holliger, 1998; Pérez del Villar *et al.*, 2003, and Chardon *et al.*, 2008). Granites are believed to be highly favorable for geological disposal of radioactive wastes (Chapman and Smellie, 1986; and Parneix, 1992). In this context, the mineralogical and geochemical analyses of the secondary mineral phases of granites alteration, particularly of clay minerals, are informative for identifying the history of the alteration processes and for determining the role of these minerals in the retention of natural radionuclides. The aim of this study is to investigate possible means of uranophane formation on the surface of clay minerals and emphasizing the relationships between alteration and migration/retention processes

affecting natural radionuclides. Moreover, the results of this study might help in understanding the geochemical behaviour of U and associated REE in conditions relevant to spent fuel disposal.

Geological Setting

The geology of Gattar area, and vicinity, has been extensively studied by many authors (El Shazly, 1970; Dardir and Abu Zied, 1972; Willis *et al.*, 1988; Salman *et al.*, 1986; El Rakaiby and Shalaby, 1992; Roz, 1994; Nossier, 1996; and Shalaby, 1996). The rock units cropping out at this area are mainly metavolcanics, granodiorites, diorites, Hammamat sediments and younger granites (Fig. 1). Gattar granitic masses are classified as hypersolvus and alkali feldspar granites (El-Sayed *et al.*, 2003). They are red to pink in color and consist mainly of orthoclase and microcline perthites, quartz, biotite and muscovite. Fluorite, zircon, apatite, titanite, galena and ilmenite are observed as accessory minerals. Chlorite, epidote, sericite, illite and kaolinite are present as alteration products of hornblende and feldspars. Based on petrographic modal analysis, Gattar granites consist mainly of quartz (26-30%), perthite (41-61%), plagioclase (3-16%), biotite (0.5-1%), muscovite (1-2%) and opaque minerals (0.5-1%). Geochemically, Gattar granites are peraluminous and could be considered as A-type granite (Moussa *et al.*, 2007).

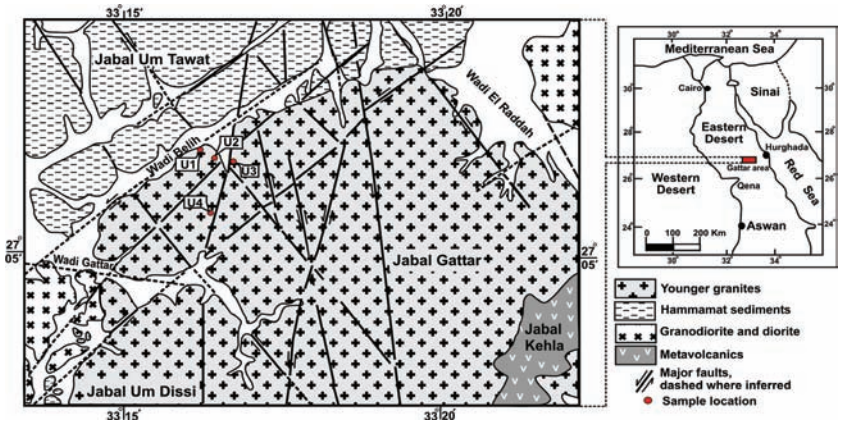

Fig. 1. Geologic map of the study area (modified from Roz, 1994).

The Hammamat sediments reach about 5 km in width and extend in a nearly east-west direction for about 20 km. They are composed mainly of conglomerates, greywackes and siltstones. These sediments are affected by alteration, including argillization, chloritization and muscovitization of lithic grains, silicification, pyritization followed by pseudomorphic oxidation and hematization. Stern and Hedge (1985) reported a Rb/Sr model age of 575 Ma for Gattar granites. However this age is younger than the $^{206}Pb/^{238}U$ crystallization ages (between 597 and 613 Ma) reported by Moussa *et al.*, (2007). On the other hand, Willis *et al.* (1988) obtained an age of 585±15 Ma for the Hammamat sediments. Presence of some xenoliths of Hammamat sediments in Gattar granites, as well as apophyses and offshoots of the granite mass into the Hammamat sediments, suggests an age younger than 585 Ma that supports the earlier 575 Ma age of Stern and Hedge (1985) and contradicts the recent 597 and 613 Ma ages of Moussa *et al.*, (2007). The latter authors interpreted the difference between these ages as multiple episodes of intrusion generated the Gattar batholith.

Faults, fractures and joints of different trends affect Gattar area. The main tectonic trends reported in the study area are: NE-SW, NNE-SSW, N-S, NW-SE and ENE-WSW (El-Sirafe and Rabie, 1989). Wadi Belih (Fig. 1) follows a major fault trending NE, more or less parallel to the local fault separating these sediments from the intruded granites to the south (Salman *et al.*, 1986; Shalaby *et al.*, 1999). Along the contact between Gattar granites and Hammamat sediments, some parts of the granites were subjected to episyenitization resulted from the hydrothermal alkaline leaching of quartz. The leaching process caused these parts to be spongy in shape.

Geology of Uranium Mineralization

During the last few decades, many uranium occurrences have been discovered in the Eastern Desert by the Egyptian Nuclear Materials Authority. Gattar granites are regarded as one of these occurrences, where surficial uranium mineralization was discovered by Salman *et al.* (1986). A few years later, several uranium occurrences within the same area have been identified (Roz, 1994; Nossier, 1996; and Shalaby, 1996). Uranium mineralization is mainly restricted to sheared tectonic contact between Gattar granites and the older Hammamat sediments. The

associated NE-SW and NNE-SSW faults and shear zones represent a pathway for the hydrothermal fluids, creating conditions favorable for alteration of Gattar granites, *e.g.* dissolving quartz, muscovitization, argillization and carbonitization. The mineralization, in the form of stains along crevices and fracture surfaces (Mahdy *et al.*, 1990), is best hosted in the Hammamat sediments near contact with sheared Gattar granites. Some mineralization may, however, occur in the hydrothermally altered parts of Gattar granites and localized within several shear and fractured zones that are filled with quartz veins (Salman *et al.*, 1986; Helmy, 1999; and El-Kammar *et al.*, 2001). Void-filling calcite have been observed in Gattar granites. Fluorite is found in significant amounts as subhedral transparent crystals. The majority of these crystals are commonly violet with blue shades. The color may reach black especially in the composite grains of fluorite and secondary uranium minerals.

The background values of uranium and thorium in the unaltered rocks range from 4.9 to 9.8 ppm U and 15 to 21 ppm Th for granites and from 5.4 to 41 ppm U and 2.8 to 6.4 ppm Th for the sediments (El-Kammar *et al.*, 2001). These values increase in altered varieties, particularly the siltstones of the Hammamat sediments, where average U reaches 4284 ppm with low Th values (average 7 ppm). Sayyah and Attawiya (1990) reported the presence of uraninite as a main primary uranium mineral in the granitic rocks. However, primary U-ores in the mineralized shear zone have not been evidenced at the surface in the recent work (*e.g.* El-Kammar, *et al.*, 2001; and Dawood, 2003), as well as the present study.

The secondary uranium minerals, represented mainly by uranophane, is detected as patches and fracture-fillings in both sheared Gattar granites and hematized Hammamat sediments (Dawood, 2003). It forms well developed needle and radiated crystals. Its color ranges from lemon yellow to straw yellow. Uranophane crystals are a few millimeters in size and occur as separate crystals or precipitated on clay minerals (Fig. 2-3).

Analytical Procedures

Four samples from the main mineralized zones of Gattar granites were collected to show variable degrees of alteration represented by

argillization and staining of reddish brown iron oxy-hydroxides. They also show surficial enrichment of yellow-colored uranium mineralization, mainly uranophane. This mineralization was scraped from the surfaces of these samples to be analyzed by electron microprobe. Some of the scraped minerals representing the four samples were isolated under binocular microscope based on their color and identified using X-Ray Diffraction (XRD). The X-ray diffractograms were made with Siemens diffractometer using Ni filter and Cu-Kα radiation at 40 kV and 20 mA. The machine is equipped with D 500 goniometer, a graphite monochrometer and a scintillation detector. The pulverized samples were scanned for about 30 minutes counting time at a rate 1 degree 2θ per half minute with step size 0.02 2θ. Peaks search and identification were performed by the DIFFRAC-AT software connected to the diffractometer. Additionally, the scraped uranyl mineralization were mounted with epoxy on glass slides then ground to the desired thickness prior to polishing. A JEOL JEE-400 vacuum evaporator was used to coat samples with a carbon layer prior to analysis. Back Scattered Electron imaging (BSE), Wavelength-Dispersion Spectral scans (WDS), X-ray compositional mapping and quantitative analyses of uranophane and associated clay minerals were performed on a JEOL JXA-8900 Electron Probe Micro Analyzer (EPMA) available at the Institute of Geosciences, University of Tübingen, Germany. The operating voltage is 15 kV, a beam diameter of 2μm and a counting time of 10-40s per element. Eighty three analyses were performed on twenty mineral grains using natural and synthetic standards of known concentrations. Setup and operating conditions of the EPMA are presented in Table 1. Data reduction for the various elements was performed by taking into account the matrix corrections between standards and samples and the analytical parameters. The matrix effects were corrected by the conventional ZAF method. Moreover, special care was taken to ensure that line overlaps were properly corrected and that background positions were clear of interfering lines among the REEs. Errors in microprobe analyses due to counting statistics are generally less than 1% in most of the analyzed elements. For REEs, where concentration <0.5%, analytical errors are higher, *i.e.* approximately 5-10%.

Table 1. Setup and operating conditions for uranophane, kaolinite and illite EPMA analyses.

Element	Line	Standard	Crystal	Bkg high (+)	Bkt low (–)	Baseline (V)	Window (V)	Bias (V)	Detection limit (ppm)
Si	Kαl	Wallastonite	PETH	5.00	5.00	0.70	9.30	1722	130
Al	Kαl	Al_2O_3	TAP	5.00	5.00	0.70	9.30	1688	150
Ca	Kαl	Wallastonite	PETJ	5.00	5.00	0.70	9.30	1700	135
U	Mαl	UO_2	PETH	5.00	5.00	0.70	9.30	1722	280
Pb	Mαl	PbF_2	PETH	5.00	5.00	0.70	9.30	1722	240
Fe	Kαl	Fe_2O_3	LIFH	5.00	5.00	0.70	9.30	1722	320
P	Kαl	$LaPO_4$	TAP	5.00	5.00	0.70	9.30	1700	235
Mg	Kαl	MgO	TAP	5.00	5.00	0.70	9.30	1688	210
K	Kαl	K-Niobate	PETJ	5.00	5.00	0.70	9.30	1686	200
Zn	Kαl	ZnO	LIF	5.00	5.00	0.70	9.30	1720	370
La	Lαl	$LaPO_4$	LIF	5.00	5.00	0.70	9.30	1720	480
Ce	Lαl	$CePO_4$	PETJ	5.00	5.00	0.70	9.30	1714	230
Pr	Lαl	$PrPO_4$	PETJ	5.00	5.00	0.70	9.30	1714	272
Sm	Lαl	$SmPo_4$	LIFH	5.00	5.00	0.70	9.30	1722	340
Eu	Lαl	$EuPO_4$	LIFH	5.00	5.00	0.70	9.30	1722	300
Gd	Lαl	$GdPO_4$	LIF	5.00	5.00	0.70	9.30	1720	360
Tb	Lαl	$TbPO_4$	LIFH	5.00	5.00	0.70	9.30	1722	320
Dy	Lαl	$DyPO_4$	LIFH	5.00	5.00	0.70	9.30	1722	370
Ho	Lαl	$HoPO_4$	LIFH	5.00	5.00	0.70	9.30	1722	330
Er	Lαl	$ErPO_4$	LIFH	5.00	5.00	0.70	9.30	1722	310
Tm	Lαl	$TmPO_4$	LIFH	5.00	5.00	0.70	9.30	1722	400
Lu	Lαl	$LuPO_4$	LIFH	5.00	5.00	0.70	9.30	1722	330

Results

The BSE imaging and X-ray maps of the scraped uranyl mineralization show association of secondary uranium and clay minerals (Fig. 2 and 3). The WDS scan shows that the principal constituents of the recognized secondary uranium mineral are U, Ca and Si, which is support

identification as uranophane. Argillic alteration has been identified by X-ray diffraction (Fig. 4) and WDS scan, where kaolinite and illite are the most abundant minerals. The WDS shows that the principal elements are Al and Si in kaolinite and Al, Si, Fe and K in illite. Minor amounts of Ca, Mg and Zn are also identified.

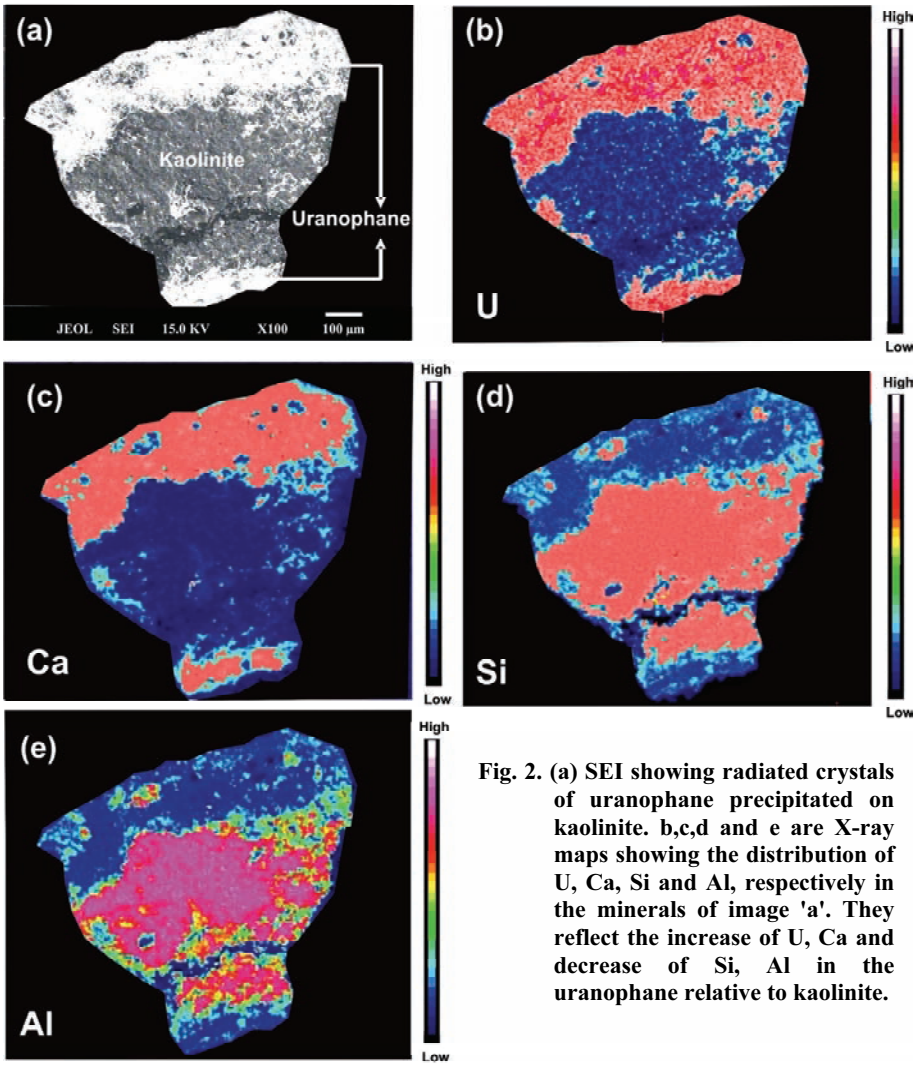

Fig. 2. (a) SEI showing radiated crystals of uranophane precipitated on kaolinite. b,c,d and e are X-ray maps showing the distribution of U, Ca, Si and Al, respectively in the minerals of image 'a'. They reflect the increase of U, Ca and decrease of Si, Al in the uranophane relative to kaolinite.

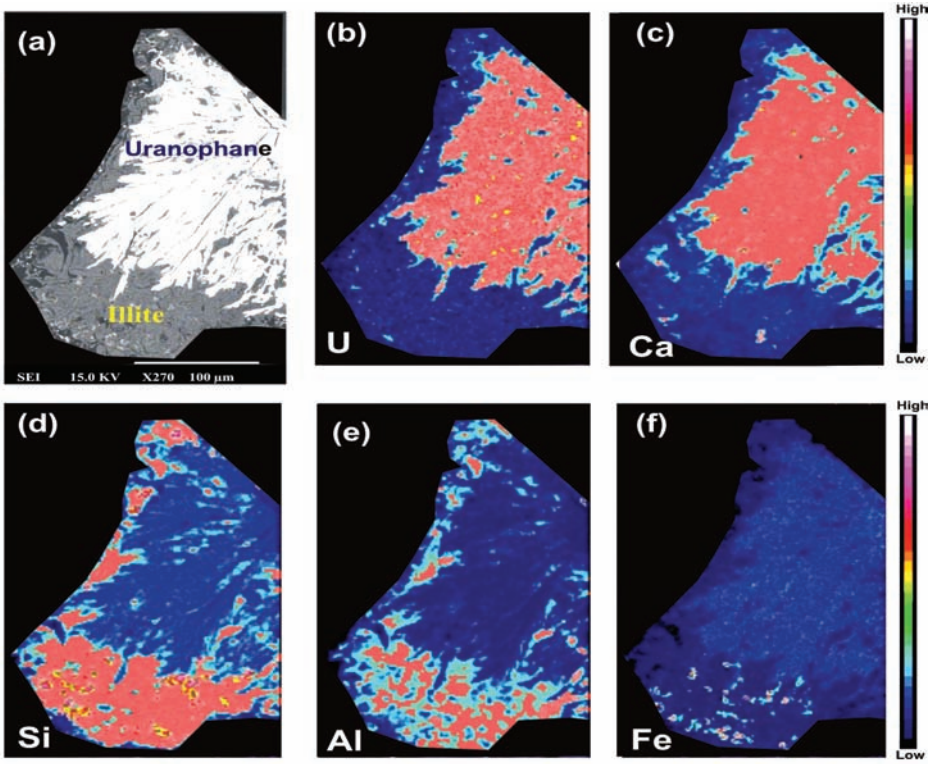

Fig. 3. (a) SEI showing radiated crystals of uranophane precipitated on illite. b,c,d,e and f are X-ray maps showing the distribution of U, Ca, Si, Al and Fe respectively in the minerals of image 'a'. They reflect the increase of U, Ca and decrease of Si, Al, Fe in the uranophane relative to illite.

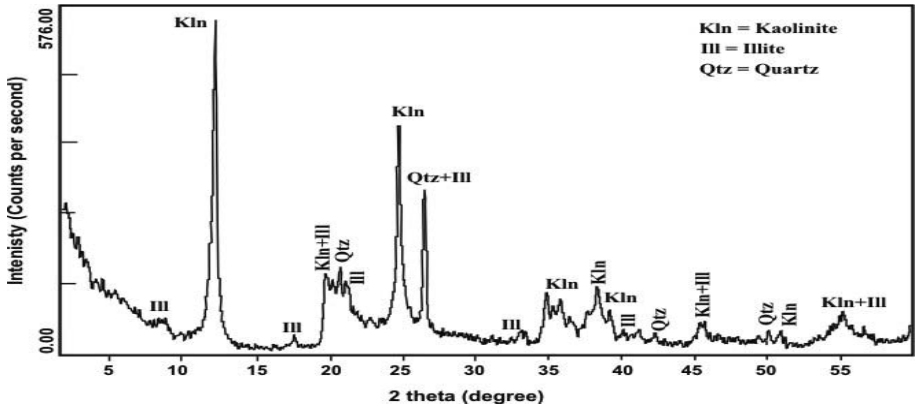

Fig. 4. X-ray diffractogram showing the peaks of kaolinite, illite and quartz as constituents of the alteration products representing sample "U2".

Uranophane Composition

The chemical composition of uranophane, determined by EPMA, is shown in Table 2. UO_3, SiO_2 and CaO are the essential constituents (66.09, 13.72, 6.42 wt.% in average, respectively), whereas P_2O_5 and Fe_2O_3 are minor constituents (0.47, 0.12 wt% in average, respectively). Insignificant amounts (<0.1 wt.%) of Al_2O_3, PbO and ZnO are also observed. The total amount of the REE varies from 0.11 to 0.71 with an average of 0.27 wt%. The proportions of U, Si and Ca are similar to the literature data, from which it would appear that Gattar uranophane is fairly typical. When the radiogenic lead accumulates in the structure of the uranium minerals, uranium content decreases concomitantly (Fayek *et al.*, 1997). The analyses of uranophane from Gattar granites show a non-significant correlation between PbO and UO_3 (Fig. 5). This reflects that Pb does not exist as a radiogenic product, a possible criterion for a young age of the uranophane. This is in agreement with the young uranium-series age (50,000-159,000 years) of uranophane from several occurrences in the Eastern Desert (Osmond *et al.*, 1999; and Dawood, 2001). These relations also suggest that Pb was carried by the same fluids that precipitated uranophane. Sources of Pb could be the previously formed galena which found as accessory mineral in granites.

Table 2. Representative EPMA data (wt.%) of uranophane, kaolinite and illite from the Gattar granites.

Sample	U1			U2			U3			U4		
	Uph	Kln	m	Uph	Kln	m	Uph	Kln	m	Uph	Kln	m
SiO_2	13.32	49.29	49.06	14.54	50.83	46.76	15.87	44.80	49.53	13.26	48.86	50.15
Al_2O_3	0.25	35.73	27.15	0.06	35.19	26.92	0.02	38.69	25.34	0.03	37.13	25.03
CaO	7.61	0.57	0.79	5.93	0.11	1.98	6.04	0.19	1.42	6.31	0.13	0.76
UO_3	67.53	0.03	b.d.	68.00	b.d.	b.d.	65.40	0.05	b.d.	65.96	b.d.	b.d.
PbO	0.02	b.d.	0.02	b.d.	b.d.	b.d.	0.02	b.d.	0.09	0.02	b.d.	b.d.
Fe_2O_3	0.49	0.03	2.02	0.07	0.13	2.16	0.02	0.08	3.40	0.03	0.04	1.49
P_3O_5	0.63	0.35	0.26	0.09	0.20	0.39	0.34	0.34	0.08	0.56	0.09	0.23
MgO	b.d.	b.d.	1.68	b.d.	b.d.	1.77	b.d.	0.06	1.62	b.d.	0.06	1.88
K_2O	b..d.	b.d.	6.36	b.d.	b.d.	7.43	b.d.	0.08	7.59	b.d.	0.06	7.32
ZnO	0.00	0.04	0.21	0.00	0.04	0.51	0.00	0.02	0.41	0.14	0.05	0.19
La_2O_3	0.071	0.081	0.062	0.062	0.05	0.05	0.06	0.087	b.d.	0.05	0.082	0.051
Ce_2O_3	0.021	0.024	0.024	b.d.	0.031	0.035	0.061	0.041	b.d.	0.030	0.041	0.034
Pr_2O_3	0.039	0.053	0.039	b.d.	0.082	0.04	0.064	0.03	0.023	0.048	b.d.	0.059
Sm_2O_3	0.033	0.035	0.031	0.041	0.03	0.03	0.04	0.031	b.d.	0.032	0.040	0.033
Eu_2O_3	0.125	0.026	0.027	0.029	0.03	0.03	0.046	0.037	b.d.	0.127	0.027	0.029
Gd_2O_3	0.080	0.042	0.045	0.046	b.d.	0.040	0.047	0.040	b.d.	0.068	0.079	b.d.
Tb_2O_3	0.036	0.030	0.037	0.036	0.032	b.d.	0.039	0.069	0.030	0.051	0.032	0.03
Dy_2O_3	0.049	0.041	0.074	0.038	0.034	0.053	0.039	0.038	0.037	0.037	0.042	0.078

Table 2. Contd.

Sample	U1			U2			U3			U4		
	Uph	**Kln**	**m**	**Uph**	**Kln**	**m**	**Uph**	**Kln**	**m**	**Uph**	**Kln**	**m**
Ho_2O_3	0.033	0.038	0.046	0.031	0.031	b.d.	0.040	0.031	b.d.	0.034	0.031	0.045
Er_2O_3	0.106	0.042	0.060	0.044	0.041	0.70	0.039	0.035	0.030	0.031	b.d.	0.033
Tm_2O_3	0.90	0.044	0.055	0.047	0.042	0.051	0.040	0.045	0.043	0.139	0.043	b.d.
Lu_2O_3	0.107	0.030	0.078	0.114	0.30	0.066	0.037	0.047	0.081	0.034	0.038	0.05
Total	**90.64**	**86.52**	**88.11**	**89.18**	**86.93**	**88.38**	**88.25**	**84.84**	**89.72**	**86.98**	**86.86**	**87.48**

U1-U4: refer to sample locations (see Fig. 1). Uph=Uranophane, Kln=Kaolinite, Ill=illite and b.d. = below detection limit.

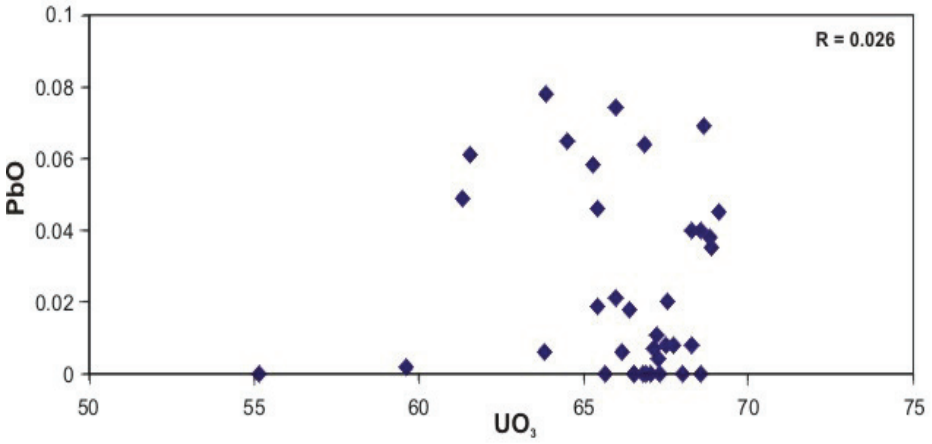

Fig. 5. PbO vs. UO_3 bivariant plot of uranophane.

Clay Minerals Composition

The chemical compositions of kaolinite and illite are shown in Table 2. For kaolinite, SiO_2 and Al_2O_3 represent the essential constituents (47.79 and 37.01 wt.% in average, respectively). The Fe_2O_3, CaO and P_2O_5 contents are generally low. Fe_2O_3 ranges from 0.015 to 0.13 wt.% with an average of 0.07 wt.% , CaO ranges from 0.08 to 0.57 wt.% with an average of 0.20 wt.% and P_2O_5 ranges from 0.09 to 0.35 wt.% with an average of 0.19 wt.%. UO_3 content in kaolinite is generally low (< 0.1 wt.%). Insignificant amounts (< 0.1 wt.%) of PbO, MgO, K_2O and ZnO are also measured. The total amount of the REE varies from 0.12 to 0.43 wt.% with an average of 0.25 wt.%.

Similar to kaolinite, SiO_2 and Al_2O_3 represent the essential constituents for illite (48.31 and 26.11 wt.% in average, respectively). Comparison in chemical composition of kaolinite and illite is shown in Fig. 6. It indicates that the illite has higher values of K_2O, MgO, Fe_2O_3, CaO, ZnO and P_2O_5, but lower value of Al_2O_3. Illite has nearly similar REE contents to kaolinite (varies from 0.23 to 0.46 wt.% with an average of 0.28 wt.%). Insignificant amount of PbO is also recorded in illite (< 0.1 wt.%). UO_3 content in illite is generally below detection limit.

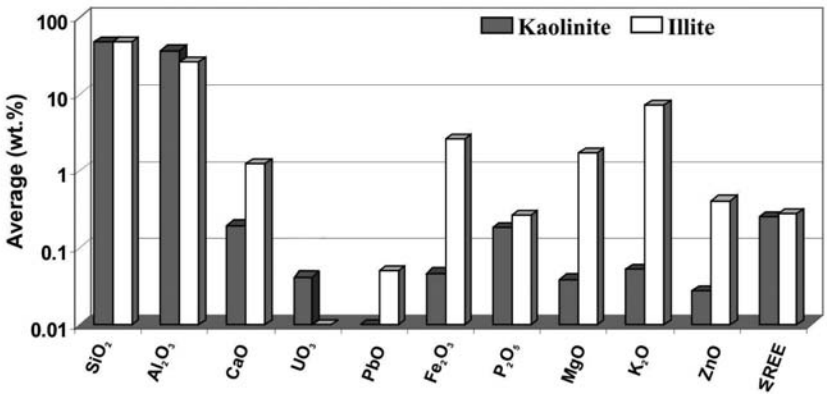

Fig. 6. Histogram comparing the chemical composition of kaolinite and illite.

REE Patterns of Uranophane and Clay Minerals

Studying the distribution of Rare Earth Elements (REE) considered as a powerful tool in identifying petrogenesis of minerals or rocks. The presence of significant values of REE within the secondary phases such as uranophane and clay minerals indicates that REE can be mobile during alteration of the host rock. Figure 7 shows the chondrite-normalized REE patterns of the uranophane, kaolinite and illite in comparison with the patterns of fresh and altered Gattar granites as reported by El Kammar *et al.* (2001). This figure suggests that incorporation of dissolved REE and U into clay minerals may result in significant modification of the REE distribution from that of the parent rocks. In general, uranophane, kaolinite and illite are higher in REE than the host granites. Both fresh and altered granites do not show significant difference in LREE concentrations, whereas slight enrichment in HREE is observed in the altered granites. Both patterns show negative Eu anomalies. On the other hand, the chondrite-normalized $(La/Lu)_N$ ratio of the uranophane,

kaolinite and illite are lower than one (varies from 0.07 to 0.12), showing HREE-enriched features. The greater values of HREE in these minerals indicate high mobility and stability of HREE in aqueous solution. This is in agreement with the findings of Biddau *et al.* (2002) who concluded that when concentrations of REE in water are normalized relative to the parent rocks, a preferential leaching of HREE into the water phase is observed. Enrichment of HREE in the altered Gattar granites due to alteration was reported by El Kammar *et al.* (2001). The muscovitization of silicates precursor and metamictization of HREE-bearing minerals such as zircon may supply the additional HREE to the altered granites (El Kammar *et al.*, 2001). Positive Eu anomalies exist in uranophane, kaolinite and illite (Fig. 7). This may indicate that solution responsible for feldspar alteration and uranophane formation was enriched in Eu^{2+}. On the other hand, the negative Eu anomaly in the fresh and altered host granitic rocks resulted from leaching of Eu^{2+} by reducing hot solutions (El Kammar *et al.*, 2001). A negative Ce anomaly is recorded in uranophane, kaolinite and illite. This anomaly may result from the precipitation of Ce^{4+} compounds (*e.g.* Ce hydroxide).

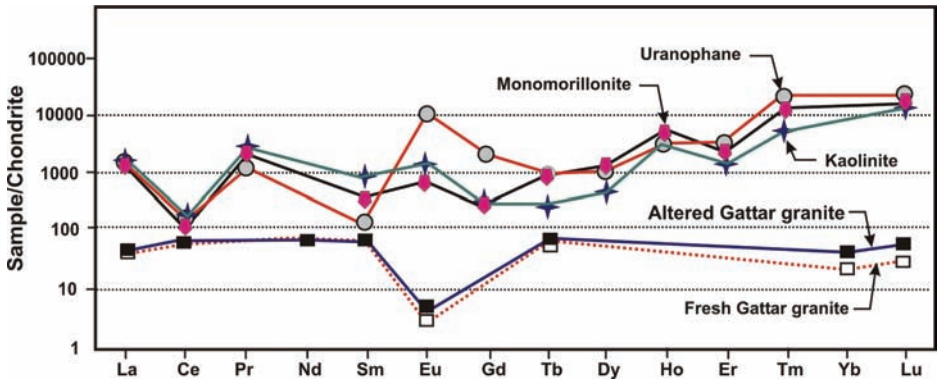

Fig. 7. Chondrite-normalized REE patterns of the uranophane, kaolinite and illite. Patterns of fresh and altered granites are from El Kammar *et al.* (2001). The REE normalization is based on the chondrite data given by Anders and Grevesse (1989).

Discussion

Uranium existing in Gattar granites can be genetically divided into two types; primary uranium and secondary uranium. The former is fixed in rocks during the crystallization of magma and was only identified as

uraninite by Sayyah and Attawiya (1990), while the latter was precipitated by various geological events from dissolved and transported uranium, which in turn, derived from the primary sources. Only uranophane has been identified in the present study as the secondary uranium mineral. However, other phases such as soddyite, tyuyamunite and schreckingerite were identified by Mahdy *et al.* (1990) and Helmy (1999). In the present work, no primary uranium mineral has been detected.

Argillic Alteration

Argillic alteration is characterized by the formation of the clay minerals by extreme base leaching of anhydrous aluminium silicates which are found in Gattar granitic rocks. The clay minerals, which form at the expense of K-feldspars and plagioclases, are represented by kaolinite and illite. Argillic alteration may be produced during hydrothermal alteration as well as by weathering under tropical or sub-tropical wet climatic conditions. McDowell and Elders (1980) suggested that argillic alteration could be formed at a low temperature below 100^{o}C. It was described as a low temperature subaerial epithermal alteration by Reed and Spycher (1985). Suto *et al.* (2007) applied an experimental approach to understand the reactions that take place upon the injection of CO_2-rich fluid into high temperature (150-250^{o}C) granite system. Their experimental work results demonstrated dissolution of plagioclase and the precipitation of clay minerals such as kaolinite and illite. Based on mineralogical and isotopic study on the El Berrocal hydrothermally altered granite (Spain), Pérez del Villar *et al.* (2003) concluded that kaolinite and illite could be formed from hydrothermal alteration of K-feldspars and plagioclases (70 and 125°C).

The origin of clay minerals developed on the shear zones of the Gattar granites may be debatable because hydrothermal activity is often associated with the late cooling of granitic plutons may also generate the conditions for extensive argillization. El-Kammar *et al.* (2001) demonstrated surficial kaolinization of feldspars in Gattar granite is due to action of meteoric water. On the other hand, association of argillic alteration in shear zones of Gattar granite with medium-temperature fluid circulation, *e.g.,* networks of quartz veinlets, may point to hydrothermal origin. Magmatic origin of hydrothermal solutions of Gattar granite has

been suggested by Helmy (1999). Based on fluid inclusion investigation, he considered that uranium mineralization at Gattar granites was formed from mixing of hot and saline magmatic fluids with low salinity meteoric water. Bearing in mind the age of 575-613 Ma for the Gattar granite (Stern and Hedge, 1985; and Moussa *et al.*, 2007) and the age of 50,000 to 159,000 years for the secondary U-mineralization in the Eastern Desert of Egypt (Osmond *et al.*, 1999; and Dawood, 2001), it is more probable that the hydrothermal fluids responsible for uranium mineralization in Gattar area have no relation to the magmatic processes which formed the host granite. Presence of secondary uranium mineralization, uranophane, on the surface of kaolinite and illite may suggest that the genesis of clay minerals is synchronous to that of the uranophane precipitation. It is postulated that both of hydrothermally aided and weathering aided alterations are very probably connected with activity of alkali high and relatively low temperature solutions and also with meteoric nature of these solutions. The numerous fractures, faults and shear zones in the Gattar granites acted as good conduits for fluids circulation of both hydrothermal alteration and weathering processes.

The role of groundwater in the formation of secondary uranium mineralization (*ca.* 100,000 year) in the Eastern Desert of Egypt has been demonstrated by many authors (Osmond *et al.*, 1999; Dawood, 2001; Dawood *et al.*, 2004; Osmond and Dabous, 2004; and Abd El-Naby, 2007). At this time, the Eastern Desert was flooded by meteoric water that could penetrate to deeper parts along faults and fracture zones of the of the Gattar pluton and could be slightly heated from radioactive decay of U, Th and K in the granites (Birch, 1954; Fehn *et al.*, 1978; and Shrier and Parry, 1982). The heated fluids started with more acidic affinity which is suitable for alteration of feldspar to kaolinite (reactions 1, 2):

$$\underset{\text{K-feldspar}}{2\,KAlSi_3O_8} + H_2O + 2\,H^+ \rightarrow \underset{\text{Kaolinite}}{Al_2Si_2O_5(OH)_4} + 2\,K^+ + \underset{\text{Silica}}{4\,SiO_2} \qquad (1)$$

$$\underset{\text{Albite}}{2\,NaAlSi_3O_8} + H_2O + H^+ \rightarrow \underset{\text{Kaolinite}}{Al_2Si_2O_5(OH)_4} + 2Na^+ + \underset{\text{Silica}}{4SiO_2} \qquad (2)$$

The physicochemical conditions of these fluids were ever changing due to consequent reactions with wall rocks. When the fluids approach the surface, passing through fracture system, the pressure decreased and

the pH increased due to the loss of volatile components (Romberger, 1984). They became alkaline and oxidizing and caused subsolidus alterations of plagioclase to illite and albite according to the following reactions:

$$2\ NaAlSi_3O_8 + \text{bicarbonate-carbonate}\ H_2O + K^+ \leftrightarrow$$

Albite

$$[K,(H_3O^+]Al_2(Si^3AlO_{10})(OH)_2 + SiO_2 + 2Na^+ + \text{Carbonate} \quad (3)$$

Illite Silica

$$CaAl_2Si_2O_8 + 4H_4SiO_4 + 2Na^+ \rightarrow 2NaAlSi_3O_8 + Ca^{2+} + 8H_2O \quad (4)$$

Anorthite polysilicic acid Albite

Evidences of the alkaline and oxidizing nature of the ascending fluids have been given by El-Kammar *et al.* (2001). These include: (1) Dissolution of quartz, (2) enrichment of the altered granite in Ca, Mg and precipitation of iron as (hydr)oxides, (3) precipitation of uranophane as secondary uranium phase, (4) hematization, pseudomorphic oxidation of pyrite and muscovitization of biotite. Furthermore, potassium released from reaction (1) was used in reaction (3) and similarly, silica released from reactions (1, 2 & 3) and Ca released from reaction (4) were probably spent in the formation of uranophane, particularly on the surface of the clay minerals.

Uranium Mobilization and Uranophane Formation

The uranium mineralization in the altered Gattar granites is controlled by shear zones in which the degree of fluid-rock interaction was very high and argillic alteration is most abundant. Clay minerals associated with the uranium mineralization along the shear zones played an important role in uranium precipitation within these parts of the granites. Alteration develops a similar pattern at regional and smaller scales, with a close relationship between the degree of alteration and the amount of structural elements observed on the shear zones (*e.g.*, faults, fractures).

The activity of carbonate in many uranium-mineralizing systems is significant as indicated from the abundance of calcite (Romberger, 1984).

Jerden and Sinha (2003) confirmed that uranyl-carbonate complexes such as $UO_2(CO_3)_2^{2-}$ and $UO_2(CO_3)$ are the most important U-complexes at pH of 7. In the presence of Ca, two of other calcium-uranyl-carbonate species, $CaUO_2(CO_3)_3^{2-}$ and $Ca_2UO_2(CO_3)_3$, are dominant aqueous species (Bernhard *et al.*, 1996&2001; Kalmykov and Choppin, 2000; Brooks *et al.*, 2003; and Kelly *et al.*, 2003). Speciation calculations obtained by Dong and Brooks (2006) indicate that $CaUO_2(CO_3)_3^{2-}$ is more important than $Ca_2UO_2(CO_3)_3$ at low Ca^{2+} concentration (e.g., <2.2 mmol/l), and that the $Ca_2UO_2(CO_3)_3$ distribution increases with increasing Ca^{2+} concentration. A neutral dicalcium uranyl tricarbonate complex [$Ca_2UO_2(CO_3)_3$] has been reported to influence the speciation of uranium in the pH region from 6 to 10 in calcium-rich uranium-mining-related water (Bernhard *et al.*, 2001). The precipitation of calcite accounts for diminishing the activity of these ternary calcium-uranyl-carbonate species beginning from pH ~8. The dominant aqueous species at these conditions, is uranyl-carbonate complex $[UO_2(CO_3)_3]^{4-}$.

Uranium could be removed from solution via: (1) Sorption onto clay minerals; (2) dissolution of feldspar, formation of clay minerals and subsequent precipitation of uranophane, or both sorption and dissolution-precipitation. Which of these reactions take place and to what extent depends mainly on various geochemical parameters such as pH, redox potential and ionic strength of the aqueous medium, speciation of the radionuclides, surface area of the mineral substrates, acidity and density of the sorption sites.

Sorption is a significant mechanism which contributes to the retention of uranium from a solution to contiguous clay minerals. Dissolved uranium will always partition itself between the water and the surfaces of contacting clay minerals. There are several mechanisms by which a sorption process can occur, for example: adsorption, absorption, ion exchange, and surface precipitation. The sorption of U(VI) on clay minerals has been investigated by numerous authors (*e.g.* Pabalan and Turner, 1997; Boult *et al.*, 1998; and Sylwester *et al.*, 2000). The possibility that U is incorporated into the kaolinite and illite structure through ion exchange can be excluded for the following reasons: 1) presence of insignificant amounts of U in both kaolinite and illite; 2) differences in ionic size between U^{6+} (1.02 A°) and cations present in kaolinite and illite structures (Si^{4+} (0.40 A°), Al^{3+} (0.53 A°), Mg(II) (0.71

A°) and Fe(III) (0.63 A°) and 3) the presence of CO_3^{2+} anions in water could form complexes with dissolved hexavalent uranium. Such complexation and hydrolysis of the uranyl cation generally precludes uranium from substitution within intracrystalline sites of the clay minerals (Pabalan and Turner, 1997; Boult *et al.*, 1998; and Payne *et al.*, 1998). Therefore, the sorption of U(VI) in the Gattar clay minerals should be low due to the presence of dissolved carbonate ions and to the slightly alkaline conditions under which U(VI) occurs as the weakly sorbed $UO_2(CO_3)_2^{2-}$ and $UO_2(CO_3)_3^{4-}$.

The only remaining possibility is that U could be removed from solution through dissolution of feldspar, formation of clay minerals and subsequent precipitation of uranophane. Nucleation of uranophane appeared to occur as a result of successful interaction between U and both of Ca and SiO_4 ions. The main source of Ca and SiO_4 is the feldspars (reactions 1-4), where the dissolution of the feldspars resulted in a diffusional gradient of Ca and SiO_4 ions away from its surface. As the uranium, calcium and silicon loading increase, nuclei of uranophane would likely form at the kaolinite and illite surface, where there was increased probability of electrostatic attraction between charged uranium and calcium cations and the negative fixed charges on clay mineral surfaces. It is possible that the Ca and Si released from feldspars alteration reacted with uranyl carbonate complexes to form a stable calcium uranyl-silicate surface species, uranophane (reaction 5).

$$4Ca^{+2}(aq) + 2UO_2(CO_3)_3^{-4}(aq) + 2H_4SiO_4(aq) + 5H_2O \leftrightarrow Ca(UO_2)_2[SiO_3(OH)]_2.5H_2O + 3CaCO_3 + 6H^+ \quad (5)$$

Uranophane Calcite

Similarities in the REE patterns of uranophane and kaolinite impose that U and REE were leached from common source (granitic rocks) and transported together as carbonate complexes to the shear zones, and then incorporated in the formation of uranophane and kaolinite. Relative to other REE, Eu as Eu^{+2} is preferentially hosted in plagioclases during magmatic processes (Alderton *et al.*, 1980) and consequently easily liberated during weathering and alteration and concentrated later to produce supergene enrichment (Lewis *et al.*, 1998; Dawood *et al.*, 2004; and Liu and Zhang, 2005). This may explain the positive Eu anomaly in the uranophane, kaolinite and illite. The negative Ce anomaly may reflect the possibility that these minerals were affected by oxic groundwater

from which Ce had been previously fractionated by Ce (IV) oxide precipitation (Jerden and Sinha, 2003). Hidaka *et al.* (2005) attributed the large chemical fractionation between Ce and other LREE to the formation of secondary minerals under oxidizing conditions.

Conclusion

Secondary uranium mineralization is dominated by uranophane which is mainly composed of UO_3, SiO_2 and CaO. Other constituents such as P_2O_5, Fe_2O_3, Al_2O_5, PbO and ZnO are present in minor amounts. Clay minerals associated with the uranium mineralization along the shear zones of the Gattar granites are represented mainly by kaolinite and illite. They played an important role in the uranium accumulation in the altered zones. SiO_2 and Al_2O_3 represent the essential constituents for kaolinite and illite. Other oxides such as CaO, Fe_2O_3, MgO, P_2O_5 are present in minor amounts. The presence of significant values of REE within the secondary phases such as uranophane and clay minerals indicate that REE can be mobilized during alteration of host rock. The chondrite-normalized REE patterns of the uranophane, kaolinite and illite show HREE-enriched features. Presence of +ve Eu^{2+} and –ve Ce^{4+} anomalies in the studied secondary phases may reflect the interaction of the Gattar granites with solutions under oxidizing condition.

In their ways along fractured granites, the deeply penetrated heated meteoric water reacted with Gattar granites and released U and REE from their accessory minerals such as monazite, apatite, zircon and uraninite. U and REE were likely transported by this hot solution as uranyl- and REE-carbonate. Presence of both calcite in association with uranophane supports this assumption. Movement of these hot solutions has been facilitated by pre-existing faults and more permeable lithological horizon (*i.e.* Hammamat sediments). Retention of uranium from a solution by clay minerals through sorption is excluded for the following reasons: 1) Presence of insignificant amounts of U in both kaolinite and illite; 2) differences in ionic size between U^{6+} and cations present in kaolinite and illite structures 3) presence of dissolved carbonacte complexes which generally precludes uranium from substitution within intracrystalline sites of the clay minerals. Alternatively, U could be removed from solution through dissolution of feldspar, formation of clay minerals and

subsequent precipitation of uranophane. It is possible that the Ca and Si released from feldspar alteration reacted with uranyl carbonate complexes to form uranophane at the kaolinite and illite surfaces.

Acknowledgements

My thanks are due to Deutscher Akademischer Austauschdienst (DAAD) for supporting my post-doctoral visit at Tübingen University, Germany. I am grateful to W. Frisch, Tübingen University for his support with laboratory facilities.

References

Abd El-Naby, H.H. (2007) Genesis of secondary uranium minerals associated with jasperoid veins, El Erediya area, Eastern Desert, Egypt, *Mineralium Deposita*, **43**: 933-944.

Akçay, H. (1998) Aqueous speciation and pH effect on the sorption behaviour of uranium by illite, *J. Radioanalytical and Nuclear Chemistry*, **237**(1-2): 133-137.

Alderton, D.H.M., Pearce, J.A. and **Potts, P.J.** (1980) Rare earth elements mobility during granite alteration: evidence from southwest England, *Earth Planet. Sci. Lett.*, **49**: 149-165.

Anders, E. and **Grevesse, N.** (1989) Abundances of the elements: Meteoritic and solar, *Geochim. Cosmochim. Acta*, **53**: 197-214.

Bernhard, G., Geipel, G., Reich, T., Amayri, S. and **Nitsche, H.** (2001) Uranyl (VI) Carbonate Complex Formation: Validation of the $Ca_2UO_2(CO_3)_3$ Species, *Radiochim. Acta*, **89**: 511-518.

Bernhard, G., Geipel, G., Brendler, V. and **Nitsche, H.** (1996) Speciation of uranium in seepage waters of a mine tailing pile studied by time-resolved laser-induced fluorescence spectroscopy (TRLFS), *Radiochim. Acta*, **74**: 87-91.

Biddau, R., Cidu, R. and **Frau, F.** (2002) Rare earth elements in waters from albite-bearing granodiorites of central Sardinia, Italy, *Chem. Geol.*, **182**: 1-14.

Birch, F. (1954) Heat from radioactivity. In: F. Henry (ed.) *Nuclear Geology*, New York: Wiley, pp: 148-174.

Boult, K.A., Cowper, M.M., Heath, T.G., Sato, H., Shibutani, T. and **Yui, M.** (1998) Towards an understanding of the sorption of U(VI) and Se(IV) on sodium bentonite, *Journal of Contaminant Hydrology*, **35**: 141-150.

Brooks, S.C., Fredrickson, J.K., Carroll, S.L., Kennedy, D.W., Zachara, J.M., Plymale, A.E., Kelly, S.D., Kemner, K.M. and **Fendorf, S.** (2003) Inhibition of Bacterial U(VI) Reduction by Calcium. Environ, *Sci. Technol.*, **37**(9): 1850-1858.

Chapman, N.A. (1994) The geologist's dilemma-predicting the future behaviour of buried radioactive wastes, *Terra Nova*, **6**: 5-19.

Chapman, N.A. and **Smellie, J.A.T.** (1986) Introduction and summary of the workshop. In: N.A. Chapman and J.A.T. Smellie (eds.) *Natural Analogues to the Conditions Around a Final Repository for High-level Radioactive Waste*, *Chem. Geol*., **55:** 167-173.

Chardon, E.S., Bosbach, D., Bryan, N.D., Lyon, I.C., Marquardt, C., Römer, J., Schild, D., Vaughan, D.J., Wincott, P.L., Wogelius, R.A. and **Livens, F.R.** (2008) Reactions of the feldspar surface with metal ions: Sorption of Pb(II), U(VI) and Np(V), and surface analytical studies of reaction with Pb(II) and U(VI), *Geochimica et Cosmochimica Acta*, 7**2**: 288-297.

Dardir, A.A. and **Abu Zeid, K.M.** (1972) Geology of the basement rocks between lat. 27°00′ and 27°30′N, Eastern Desert, *Annals of Geological Survey of Egypt*, **11**: 129-159.

Dawood, Y.H. (2003) Chemical composition of uranophane associated with peraluminous granite, north Eastern Desert of Egypt, *M.E.R.C. Ain Shams Univ., Earth Sci. Ser.*, **17**: 43-57.

Dawood, Y.H. (2001) Uranium-series disequilibrium dating of secondary uranium ore from south Eastern Desert of Egypt, *Appl. Radiat. Isotopes*, **55**(6): 881-887.

Dawood, Y.H., Abd El-Naby, H.H. and **Sharafeldin, A.A.** (2004) Influence of the alteration processes on the origin of uranium and europium anomalies in trachyte, central Eastern Desert, Egypt, *J. Geochem. Explo.*, **88**: 15-27.

Dong, W. and **Brooks, S.C.** (2006) Termination of the formation constants of ternary complexes of uranyl and carbonate with alkaline earth metals (Mg^{2+}, Ca^{2+}, Sr^{2+} and Ba^{2+}) using anion exchange method, *Environ Sci Technol.*, **40**(15): 4689-95.

El Rakaiby, M.L. and **Shalaby, M.H.** (1992) Geology of Gabal Gattar batholith, Central Eastern Desert, Egypt, *International Journal of Remote Sensing*, **13**: 2337-2347.

El Shazly, E.M. (1970) Evolution of granitic rocks in relation to major tectonic, *The West Commemoration*, **11**: 569-581.

El-Kammar, A.M., Salman, A.E., Shalaby, M.H. and **Mahdy, A.I.** (2001) Geochemical and genetical constraints on rare metals mineralization at the central Eastern Desert of Egypt, *Geochem. J.*, **35** (2): 117-135.

El-Sayed, M.M., Shalaby, M.H. and **Hassanen, M.A.** (2003) Petrological and geochemical constraints on the tectonomagmatic evolution of the late Neoproterozoic granitoid suites in the Gattar area, north Eastern Desert, Egypt, *N. Jb. Miner. Abh.*, **178**: 239-275.

El-Sirafe, A.M. and **Rabie, S.J.** (1989) Contribution of aeromagnetic to structural mapping of Gebel Gattar area, north Eastern Desert, Egypt, *J. Afric. Earth Sci.*, **10** (3): 132-155.

Fayek, M., Janeczek, J. and **Ewing, R.C.** (1997) Mineral chemistry and oxygen isotopic analyses of uraninite, pitchblende and uranium alteration minerals from the Cigar Lake deposit, Saskatchewan, Canada, *Appl. Geoch.*, **12**: 549-565.

Fehn, U., Cathles, L.M. and **Holland, H.D.** (1978) Hydrothermal convection and uranium deposits in abnormally radioactive plutons, *Econmic Geology*, **73**: 1556-1566.

Gaskova, O.L. and **Bukaty, M.B.** (2008) Sorption of different cations onto clay minerals: Modelling approach with ion exchange and surface complexation, *Physics and Chemistry of the Earth*, **33** (14-16): 1050-1055.

Helmy, H.M. (1999) Mineralogy, fluid inclusions and geochemistry of the molybdenum-uranium-fluorite mineralizations, Gebel Gattar area, Eastern Desert, Egypt, *Intern. Conf. on Geochemistry, Alexandria University*, 15-16 Sept. 1999: 171-198.

Hidaka, H. and **Holliger, P.** (1998) Geochemical and neutronic characteristics of the natural fossil fission reactors at Oklo and Bangombé, Gabon, *Geochim. Cosmochim. Acta*, **62**: 89-108.

Hidaka, H., Janeczek, J., Skomurski, F.N., Ewing, R. and **Gauthier-Lafaye, F.** (2005) Geochemical fixation of rare earth elements into secondary minerals in sandstones beneath a natural fission reactor at Bangombé, Gabon, *Geochim. Cosmochim. Acta*, **69**(3): 685-694.

Jerden, J.L. Jr. and **Sinha, A.K.** (2003) Phosphate based immobilization of uranium in an oxidizing bedrock aquifer, *Appl. Geochem.*, **18**(6): 823-843.

Kalmykov, S.N. and **Choppin, G.R.** (2000) Mixed $Ca^{2+}/UO_2^{2+}/CO_3^{2-}$ complex formation at different ionic strengths, *Radiochim. Acta.*, **88**: 603-606.

Kelly, S., Kemner, K.M., Brooks, S.C., Fredrickson, J.K., Kennedy, D.W., Zachara, J.M., Fendorf, S., Plymale, A. and **Carroll, S.L.** (2003) Direct evidence for $Ca\text{-}UO_2\text{-}CO_3$ complexation, *Abstracts of Papers of ACS*, **225, U256**.

Lewis, A.J., Komninou, A., Yardley, B.W.D. and **Palmer, M.R.** (1998) Rare earth element speciation in geothermal fluids from Yellowstone National Park, Wyoming, USA. Geochim, *Cosmochim. Acta*, **62**(4): 657-663.

Liu, C. and **Zhang, H.** (2005) The lanthanide tetrad effect in apatite from the Altay No. 3 pegmatite, Xingjiang, China: an intrinsic feature of the pegmatite magma, *Chem. Geol.*, **214**: 61-77

Mahdy, M.A., Salman, A.B. and **Mahmoud, A.H.** (1990) Leaching studies on the uraniferous Hammamat sediments, Wadi Bali, Northern Eastern Desert, Egypt. Egypt, *Congress of Mining and Metallurgy 14th, Edinburgh Scotland*: 229-235.

McDowell, S.D. and **Elders, W.A.** (1980) Authigenic layer silicate minerals in borehole Elmore 1, Salton Sea geothermal field, California, USA, *Contributions to Mineralogy and Petrology*, **74**: 293-310.

Meunier, A.B. and **Velde, L.G.** (1998) The reactivity of bentonites: a review. An application to clay barrier stability for nuclear waste storage, *Clay Miner.*, **33**: 187-196.

Moussa, E.M., Stern, R.J., Manton, W.I. and **Ali, K.A.** (2007) SHRIMP zircon dating and Sm/Nd isotopic investigations of Neoproterozoic granitoids, Eastern Desert, Egypt, *Precambrian Research*, **160**: 341-356.

Nossier, L.M. (1996) U-F bearing episyenitized "desilicified" granitic rocks of Gabal Gattar, north Eastern Desert, Egypt, *Egyptian Academy of Sciences*, **46**: 375-396.

Osmond, J.K. and **Dabous, A.A.** (2004) Timing and intensity of groundwater movement during Egyptian Sahara pluvial periods by U-series analysis of secondary U in ores and carbonates, *Quaternary Res.*, **61**: 85-94.

Osmond, J.K., Dabous, A.A. and **Dawood, Y.H.** (1999) U series age and origin of two secondary uranium deposits, central Eastern Desert, Egypt, *Econ. Geol.*, **94**: 273-280.

Pabalan, R.T. and **Turner, D.R.** (1997) Uranium(6+) sorption on illite: experimental and surface complexation modelling study, *Aquatic Geochemistry*, **2**: 203-226.

Parneix, J.C. (1992) Effects of hydrothermal alteration on radioelement migration from a hypothetical disposal site for High-Level Radioactive-Waste—example from the Auriat granite, France, *Appl. Geochem.*, **7**: 253-268.

Payne, T.E., Lumpkin, G.R. and **Waite, T.D.** (1998) Uranium^{VI} adsorption on model minerals: controlling factors and surface complexation modeling. In: E.A. Jenne (Ed.) *Adsorption of Metals by Geomedia: Variables, Mechanisms and Model Applications*, San Diego: Academic Press, 75-97.

Pérez del Villar, L., Reyes, E., Delgado, A., Núñez, R., Pelayo, M. and **Cózar, J.S.** (2003) Argillization processes at the El Berrocal analogue granitic system (Spain): mineralogy, isotopic study and implications for the performance assessment of radwaste geological disposal, *Chemical Geology*, **193**: 273-293.

Reed, M.H. and **Spycher, N.F.** (1985) Boiling, cooling, and oxidation in epithermal systems: A numerical modelling approach, *Reviews in Economic Geology*, **2**: 249-272.

Romberger, S.B. (1984) Transportation and deposition of uranium in hydrothermal systems at temperatures up to 300°C: Geological implications. In: B.D Vivo., F.I.G Capaldi. and P.R. Simpson (Eds.) *Uranium Geochemistry, Mineralogy, Geology, Exploration and Resources*, London: Institution of Mining and Metallurgy, 12-17.

Roz, M.E. (1994) Geology and uranium mineralization of Gabal Gattar, north Eastern Desert, Egypt. *M.Sc. Thesis*, Cairo University, 175 p.

Salman, A.B., El Aassy, I.E. and **Shalaby, M.H.** (1986) New occurrence of uranium mineralization in Gabal Gattar, north Eastern Desert, Egypt, *Annals of Geological Survey of Egypt*, **XVI**: 31-34.

Sayyah, T.A. and **Attawiya, M.Y.** (1990) Contribution of mineralogy of uranium occurrence of Gebel Gattar granites, Eastern Desert, Egypt. Arab, *J. Nucl. Sci. Appl.*, **23**(1): 171-184.

Shalaby, M.H. (1996) Structural controls of uranium mineralization at Gabal Gattar, north Eastern Desert, Egypt, *Egyptian Academy of Sciences*, **46**: 521-536.

Shalaby, M.H., Salman, A.B., El-Kammar, A.M. and **Mahdy, A.I**. (1999) Uranium mineralization in the Hammamat sediments of the Gattar area, Northeastern Desert, Egypt, *4th Inter. Conf. Geochem., Alexandria Univ.*: 101-121.

Shrier, T. and **Parry, W.T.** (1982) A hydrothermal model for the North Canning uranium deposit, Owl Creek Mountains, Wyoming, *Economic Geology*, **77**: 632-645.

Stern, R.J. and **Hedge, G.E.** (1985) Geochronologic and isotopic constraints on Late Precambrian crustal evolution in the Eastern Desert of Egypt, *Amer. J. Sci.*, **285**: 97-127.

Suto, Y., Liu, L., Yamasaki, N. and **Hashida, T.** (2007) Initial behavior of granite in response to injection of CO_2-saturated fluid, *Applied Geochemistry*, **22**: 202-218.

Sylwester, E.R., Hudson, E.A. and **Allen, P.G.** (2000) The structure of uranium (VI) sorption complexes on silica, alumina, and illite, *Geochimica et Cosmochimica Acta*, **64**: 2431-2438.

Wazne, M., Korfiatis, G.P. and **Meng, X.** (2004) Removal of uranium from water by nanocrystalline titanium dioxide, *Protection and Restoration of the Environment*, **VII**, Mykonos, Greece: 1-9.

Willis, K.M., Stern, R.J. and **Clauer, N.** (1988) Age and geochemistry of late Precambrian sediments of Hammamat series from the north of Eastern Desert of Egypt, *Precambrian Research*, **42**: 173-187.

دور التغاير الطيني في ترسيب اليورانوفين بنطق القص للصخور الجرانيتية لجبل جتار، الصحراء الشرقية، مصر

حمدي حامد عبد النبي

هيئة المواد النووية، ص.ب. ٥٣٠ المعادي، القاهرة، مصر

المستخلص. تمت دراسة كيفية ترسيب اليورانوفان بنطق التغاير بالصخور الجرانيتية لجبل جتار عن طريق استخدام تقنيات حيود الأشعة السينية، والمسبار الإلكتروني في التعرف، على معادن اليورانوفين، والكاولينيت، والإليت المفصولة من نطق التغاير، عن طريق التصوير بواسطة الإلكترونات المبعثرة للخلف، والمسح الطيفي للأطوال الموجية المشتته والتخريط التركيبي بأشعة أكس، بالإضافة إلى التحليل الكمي لقياس التركيب الكيميائي لتلك المعادن. ترتبط تمعدنات اليورانيوم بنطق القص بزيادة درجة التغاير الطيني الناتج عن تفاعل المحاليل والصخر. يلعب التغاير الطيني، ممثلاً في الكاولينيت والإليت، دوراً هاماً في ترسيب اليورانيوم ببعض الأماكن بالصخور الجرانيتية لجبل جتار. يدل وجود الفلوريت والكالسيت بصحبة اليورانوفين، كمعادن مالئة للفراغات بنطق التغاير بالصخور الجرانيتية لجبل جتار، على احتمالية انتقال اليورانيوم في صورة معقدات كربونات اليورانيوم. لم تلعب عملية امتصاص اليورانيوم بواسطة المعادن الطينية دوراً هاماً في تكوين اليورانوفين، ويرجع ذلك إلى تشبع المحاليل بالكربونات الذائبة، حيث يوجد اليورانيوم في صورة معقد الكربونات $UO_2(CO_3)_3^{4-}$ والذي يصعب امتصاصه بالمعادن الطينية تحت ظروف وسط قلوي. التفسير الآخر هو أنه تم استخلاص اليورانيوم من المحاليل

الحاملة له أثناء عمليات انحلال للفلسبار وتكون المعادن الطينية وترسيب اليورانوفين. أدى انحلال الفلسبار إلى انتشار أيوني الكالسيوم والسيليكا بعيداً عن أسطحه مما يعطي الفرصة إلى تكوّن معدن اليورانوفين بالقرب من تلك الأسطح، حيث تزداد احتمالية تصادم أيونات اليورانيوم مع أيونات الكالسيوم والسيليكا. يتم ترسيب اليورانوفين على أسطح المعادن الطينية عند زيادة تركيز اليورانيوم في المحاليل.